Comparative Metabolome and Transcriptome Analyses of Susceptible Asparagus officinalis and Resistant Wild A. kiusianus Reveal Insights into Stem Blight Disease Resistance.

doi: 10.1093/pcp/pcaa054

Title: **Comparative metabolome and transcriptome analyses of susceptible *Asparagus officinalis* and resistant wild *A. kiusianus* revealed insights into stem blight disease resistance**

Running Title: Insights into *Phomopsis* resistance in *Asparagus*

Subject areas:

1-Environmental and stress responses

2- Regulation of gene expression

***Corresponding authors:**

Tel: +81-857-21-7213; E-mail meettoo2000@tottori-u.ac.jp (Mostafa Abdelrahman),

Tel: +81-45-503-9593; E-mail: tranplamson@duytan.edu.vn; son.tran@riken.jp (L.-S.P. Tran), and

Tel: +81-22-217-5725; E-mail kanno@ige.tohoku.ac.jp (Akira Kanno)

Number of Tables: 1

Number of black and white figures: 1

Number of colored figures: 6

Supplementary materials: 9 Tables and 1 figure

Comparative metabolome and transcriptome analyses of susceptible *Asparagus officinalis* and resistant wild *A. kiusianus* revealed insights into stem blight disease resistance

Mostafa Abdelrahman[1,2,3,*], Ryo Nakabayashi[4], Tetsuya Mori[4], Takao Ikeuchi[5], Mitsutaka Mori[5], Kyoko Murakami[5], Yukio Ozaki[6], Masaru Matsumoto[7], Atsuko Uragami[8], Hisashi Tsujimoto[2], Lam-Son Phan Tran[9,10]*, Akira Kanno[3,*]

Authors' affiliations

[1]Botany Department, Faculty of Sciences, Aswan University, Aswan 81528, Egypt

[2]Arid Land Research Center, Tottori University, Tottori 680-0001, Japan

[3]Graduate School of Life Sciences, Tohoku University, Sendai 980-8577, Japan

[4]Metabolomics Research Group, RIKEN Center for Sustainable Resource Science, 1-7-22, Suehiro-cho, Tsurumi, Yokohama 230-0045, Japan

[5]Kagawa Prefectural Agricultural Experiment Station, 1534-1 Ayagawa, Ayauta, Kagawa, 761-2306, Japan

[6]Faculty of Agriculture, Kyushu University, Fukuoka, 819-0395, Japan

[7]Institute of Tropical Agriculture, Kyushu University, Fukuoka, 819-0395, Japan

[8]Institute of Vegetable and Floriculture Science, NARO, Tsukuba, Ibaraki, 305-8519, Japan

[9]Institute of Research and Development, Duy Tan University, 03 Quang Trung, Da Nang, Vietnam

[10]Stress Adaptation Research Unit, RIKEN Center for Sustainable Resource Science, Tsurumi, Yokohama 230-0045, Japan

Abstract

Phomopsis asparagi is one of the most serious fungal pathogens, which causes stem blight disease in *Asparagus officinalis* (AO), adversely affecting its production worldwide. Recently, development of novel asparagus varieties using wild *Asparagus* genetic resources with natural *P. asparagi* resistance has become a priority in Japan due to the lack of resistant commercial AO cultivars. In the present study, comparative metabolome and transcriptome analyses of susceptible AO and resistant wild *A. kiusianus* (AK) 24 and 48 h post-inoculated (AOI_24 hpi, AOI_48 hpi, AKI_24 hpi and AKI_48 hpi, respectively) with *P. asparagi* were conducted to gain insights into metabolic and expression changes associated with the AK species. Following the infection, the resistant wild AK showed rapid metabolic changes with increased levels of flavonoids and steroidal saponins, and decreased asparagusic acid glucose ester content, compared with the susceptible AO plants. Transcriptome data revealed a total of 211 differentially expressed genes (DEGs) as the core gene set that displayed upregulation in the resistant AK versus susceptible AO after infection with *P. asparagi*. KEGG pathway analysis of these DEGs identified 11 significantly enriched pathways, including flavonoid biosynthesis and primary metabolite metabolism, in addition to plant signaling and defense-related pathways. In addition, comparative SNP and Indel distributions in susceptible AO and resistant AK plants were evaluated using the latest *A. officinalis* reference genome Aspof.V1. The data generated in this study are important resources for advancing the *Asparagus* breeding programs, and for investigations of genetic linkage map, phylogenetic diversity and plant defense-related genes.

Keywords: *Asparagus*, Insertion/deletion; Metabolome; *Phomopsis* disease, Single nucleotide polymorphism; Salinity stress, Transcriptome.

Introduction

Asparagus officinalis is an important horticultural crop, which is widely cultivated and prized for its nutritional and medicinal properties (Negi et al. 2010; Takahashi et al. 2019). The continuous increase in global population combined with frequent disease incidence in horticultural crops due to global warming will push agricultural production and food sustainability to the limit in the near future (Roos et al. 2011; Abdelrahman et al. 2017c; Abdelrahman et al. 2019b). Stem blight disease caused by *Phomopsis asparagi* (Sacc.) is one of the major fungal diseases, threatening asparagus crop production in many countries (Takeuchi et al. 2017). To control *P. asparagi*, farmers routinely apply fungicides that increase environmental burdens and financial pressure on farmers (Cheah and Horlock 2007; Yang et al. 2016). In contrast, the cultivation of new asparagus varieties with durable resistance to *P. asparagi* is a more economical and sustainable approach for controlling the extent of stem blight disease. Unfortunately, extensive screening of many commercial *A. officinalis* cultivars has not identified any reliable resistant varieties (Takeuchi et al. 2017). Therefore, the development of novel asparagus varieties with stem blight disease resistance has become a priority for the breeding community (Zaw et al. 2017; Die et al. 2018; Thao and Dung 2019).

Although wild *Asparagus* species represent a potential genetic resource for the development of disease-resistant *Asparagus* germplasm, crosses between resistant wild *Asparagus* species and cultivated *A. officinalis* did not resulted in much success in earlier time due to their distant genetic relationship (Sonoda et al. 2001). Later on, Ito et al. (2011), Kubota et al. (2012) and Iwato et al. (2014) reported that *A. kiusianus*, a wild diploid species endemic to the coastal region of the Sea of Japan and cross-compatible with *A. officinalis*, showed close genetic relationship with cultivated *A. officinalis* and exhibited strong resistance to stem blight disease. In addition, the interspecific F_1 hybrids and backcross (BC_1) progenies derived from female parent *A. officinalis* ('Mary Washington 500W', susceptible) × male parent *A. kiusianus* (AK0501, resistant) were successfully achieved, showing high stem blight disease resistance characteristics compared with *A. officinalis* (Takeuchi et al. 2017). These results suggested that wild *A. kiusianus* is an important breeding partner for the production of stem blight disease-resistant asparagus cultivars. However, the physiological and molecular mechanisms underlying stem blight resistance in *A. kiusianus* remain unknown.

Metabolomic studies have demonstrated that the abundances and structure of metabolites in plants can cause large quantitative and qualitative variations in phenotypes among cultivars and species (Matsuda et al. 2015, Abdelrahman et al., 2019a). Thus,

deciphering the metabolic regulation of the stem blight disease resistance is a necessary step toward practical strategies that ultimately enable in-depth understanding and efficient control of yield losses in *A. officinalis*. In our previous study (Abdelrahman et al. 2017b), transcriptome and phytohormonal analyses allowed us to recognize the importance of jasmonic acid biosynthesis and signaling pathways in *A. kiusianus* resistance against stem blight disease; however, the downstream metabolic changes involved in this process still remain elusive. Recent reports demonstrated that flavonoids and steroidal saponins are the major bioactive compounds in wild and cultivated *Asparagus* with potent antioxidant and antimicrobial properties (Srivastava et al. 2018; Yi et al. 2019). Thus, in the present study, we carried out comparative metabolome and transcriptome analyses of susceptible *A. officinalis* 'Mary Washington 500W' and resistant wild *A. kiusianus* (AK0501 accession) 24 and 48 h post-inoculated (hpi) with *P. asparagi* to pinpoint mechanistic insights into the metabolic changes and molecular signatures underlying stem blight disease resistance of *A. kiusianus*. In addition, we investigated comparative distributions of single nucleotide polymorphism (SNP) and insertion/deletion (Indel) in susceptible *A. officinalis* and resistant wild *A. kiusianus* to generate useful genetic markers as a powerful tool for constructing high-resolution genetic map and analyzing genetic diversity. Our findings provide comprehensive information on metabolome and transcriptome dynamics, which would be a major step for understanding the mechanisms associated with *P. asparagi* disease resistance at metabolic and genetic levels, and for accelerating the development of *asparagus*-resistant varieties using marker-assisted selection.

Results

Comprehensive metabolite profiles and network correlations in resistant wild *A. kiusianus* and susceptible cultivated *A. officinalis* in response to *P. asparagi* infection

Stem samples taken from *A. officinalis* (AO) and *A. kiusianus* (AK) plants 24 and 48 hpi with *P. asparagi* (AOI_24 hpi, AOI_48 hpi, AKI_24 hpi and AKI_48 hpi, respectively) and non-inoculated control ones (AOC and AKC, respectively) were subjected to a non-targeted metabolome analysis using liquid chromatography-quadrupole time-of-flight-tandem-mass spectrometry (LC-Q-TOF-MS). First, the mass-to-charge (*m*/*z*) values of the molecular ions of interest that changed between examined samples were selected and searched against database(s). The metabolites having molecular weights within the range of the query *m*/*z* values were then retrieved as assigned metabolites. Accordingly, a metabolome dataset composed of 1483 negative and 1239 positive ion mode metabolite signals (peaks) was

generated (Tables S1 and S2). Principal component analysis (PCA) of these metabolite signal intensities clearly showed relevant metabolic variations in resistant AKI_24 hpi and AKI_48 hpi in comparison with AKC, AOC, AOI_24 hpi and AOI_48 hpi plants (Fig. 1A-B; Fig. S1). Most of the variations in the metabolite variables in the examined *Asparagus* species were captured by PC1 (82.1 and 64.0%), where AKI_24 hpi and AKI_48 hpi were positively loaded (Fig 1A-B; Fig. S1), while the lower proportions of variances (5.7 and 12.8%) were captured by PC2 (Fig 1A-B; Fig. S1). However, the metabolite signals assigned based on the similarity to the *m*/*z* values are not always unique, due to the presence of many isomers and the limited accuracy of mass spectrometers (Xiao et al. 2012). Thus, the authentic standard compounds corresponding to these assigned metabolite signals were then subjected to a tandem mass spectrometry (MS/MS) along with the examined samples to verify the identities of the metabolites by comparing the obtained MS/MS spectra and retention times (RTs). In total, 14 metabolites were identified and annotated in 18 examined samples on the basis of MS/MS spectra, exact mass values and RTs of standards and MassBank (http://www.massbank.jp/) (Fig. 2A; Table S3).

Next, Student's *t*-test and fold change (FC ≥ 2.0 or FC ≤ 0.5; $P < 0.05$) cutoffs were implemented to identify differentially produced metabolites (DPMs) in the examined *Asparagus* species in response to *P. asparagi*, and out of the 14 assigned metabolites, 13 [except Furostan-triol-Hex-dHex-Hex (C10)] metabolites were differentially produced in at least one of nine comparisons based on these preset criteria (Table S3). In general, most of the DPMs (11 out of 13) were found in the inoculated-resistant wild 'AKI/AKC' comparison, whereas none of the DPMs were detected in the inoculated-susceptible 'AOI/AOC' (0 DPM) comparison (Fig. 2B; Table S3). Specifically, 0 and 9 metabolites increased (FC ≥ 2.0; $P <$ 0.05), while 2 and 2 metabolites decreased (FC ≤ 0.5; $P < 0.05$) in the 'AKI_24 hpi/AKC' and 'AKI_48 hpi/AKC' comparisons, respectively (Fig. 2B; Table S3). On the other hand, no DPMs were found in the susceptible 'AOI_24/AOC' and 'AOI_48 hpi/AOC' comparisons (Fig. 2B; Table S3). In addition, 3 and 9 metabolites increased, while 2 and 2 metabolites decreased in 'AKI_24 hpi/AOI_24 hpi' and 'AKI_48 hpi/AOI_48 hpi' comparisons, respectively (Fig. 2B; Table S3). These results indicated that significant and rapid metabolic changes occurred in the resistant wild AK during the infection with *P. asparagi*, contributing to stem blight disease resistance phenotype of the AK species. Heatmap clustering of all 14 identified metabolites provided additional support for our findings, where AKI_24 hpi and AKI_48 hpi were clustered in one group, whereas AKC, AOC, AOI_24 hpi and AOI_48 hpi in another group (Fig. 2C). Anthocyanin and flavone-related metabolites [cyanidin-hex-dhex-

hex (C1), cyanidin 3-rutinoside (C4), idaeins (C7 and C8), 5,6,7,4'-tetrahydroxy-8-methoxyisoflavone-hex (C12)] and saponins [protodiosin (C9) and furost-ene-triol-hex-dhex-hex (C13)] exhibited higher accumulations, whereas asparagusic acid glucose esters (C2 and C3) displayed lower accumulation in resistant wild AKI than susceptible AOI plants in response to *P. asparagi* infection (Fig. 2C-D; Table S3). Metabolite-metabolite correlation network analysis demonstrated high positive correlations between C7 and C8 ($r = 0.99$), and C7 and C12 ($r = 0.99$) (Fig. 2E). On the other hand, both asparagusic acid glucose esters C2 and C3, which decreased in both 'AKI_24 hpi/AKC' and 'AKI_48 hpi/AKC' (Table S3), showed negative correlations with the other metabolites (Fig. 2E). Similarly, genotype-genotype correlation analysis revealed high positive relationships between AKI_24 hpi and AKI_48 hpi ($r = 0.99$), AKC and AKI_24 hpi ($r = 0.92$), and AKC and AKI_48 hpi ($r = 0.88$) (Fig. 2F), while it showed a weak correlation between AKI_24 hpi and AOI_24 hpi ($r = 0.25$), and a negative correlation between AKI_48 hpi and AOI_48 hpi ($r = -0.038$) (Fig. 2F). In summary, our findings indicated that flavonoids and saponins play a major role in the stem blight disease resistance in wild AK plants, while susceptible AO plants did not exhibit significant metabolic changes.

Differential gene expression analysis of AO and AK plants in response to *P. asparagi* infection

The raw sequences derived from RNA-sequencing (RNA-seq) of 18 AO and AK samples were obtained as described in Abdelrahman et al. (2018). After removing adaptors and low-quality reads, 80.58 and 73.04% of high-quality reads (Q scores > 30) derived from AO and AK sequences, respectively, were successfully mapped to the recently released *A. officinalis* transcript reference (Aspof.V1) (Harkess et al. 2017) using Bowtie2 v.2.1.0 (Table 1). False discovery rate (FDR < 0.05) and FC (FC ≥ 2.0 or FC ≤ 0.5) were used as the minimum cutoffs to determine differentially expressed genes (DEGs) in 'AOI_24 hpi/AOC', 'AOI_48 hpi/AOC', 'AKI_24 hpi/AKC' and 'AKI_48 hpi/AKC' comparisons (Tables S4-S5). In total, 851 and 1295 upregulated (FC ≥ 2.0; FDR < 0.05) and 721 and 1430 (FC ≤ 0.5; FDR < 0.05) downregulated genes were identified in 'AOI_24 hpi/AOC' and 'AOI_48 hpi/AOC' comparisons, respectively (Fig. 3A, Tables S4). Furthermore, 214 and 331 upregulated, and 640 and 690 downregulated genes were identified in 'AKI_24 hpi/AKC' and 'AKI_48 hpi/AKC' comparisons, respectively (Fig. 3A, Table S5). In addition, we also identified the DEGs in 'AKI_24 hpi/AOI_24 hpi' and 'AKI_48 hpi/AOI_48 hpi' to gain an insight into the transcriptome changes between the two *Asparagus* species (Table S6). 2716 and 2938

upregulated, and 3800 and 3092 downregulated genes were identified in 'AKI_24 hpi/AOI_24 hpi' and 'AKI_48 hpi/AOI_48 hpi' comparisons, respectively (Fig. 3A; Tables S6 and S7).

Next, Venn diagram analysis was carried out to identify the overlapping DEGs between 'AKI/AKC' and 'AKI/AOI' comparisons (Fig. 3B). 123 upregulated and 314 downregulated genes were overlapping between 'AKI_24 hp/AKC' and 'AKI_48 hpi/AKC' comparisons (Fig. 3B). Furthermore, 10 upregulated and 52 downregulated genes were shared by 'AKI_24 hpi/AKC' and 'AKI_24 hpi/AOI_24 hpi' comparisons, while 40 upregulated and 73 downregulated genes were common in both 'AKI_48 hpi/AKC' and 'AKI_48 hpi/AOI_48 hpi' comparisons (Fig. 3B). Similarly, 8 and 28 upregulated and downregulated genes, respectively, were overlapping among 'AKI_24 hpi/AKC', 'AKI_48 hpi/AKC' and 'AKI_24 hpi/AOI_24 hpi', whereas 22 and 16 upregulated and downregulated genes, respectively, were shared by 'AKI_24 hpi/AKC', 'AKI_48 hpi/AKC' and 'AKI_48 hpi/AOI_48 hpi' (Fig. 3B). In addition, 36 and 196 upregulated and downregulated genes, respectively, were overlapping among 'AKI_24 hpi/AKC', 'AKI_48 hpi/AKC', 'AKI_24 hpi/AOI_24 hpi' and'AKI_48 hpi/AOI_48 hpi' comparisons (Fig. 3B). On the basis of the Venn diagram analysis, 211 DEGs, which were upregulated in AKI_24 hpi and/or AKI_48 hpi (e.g. 'AKI_24 hpi/AKC' and/or 'AKI_48/AKC' comparisons) (Table S5), but downregulated in susceptible AOI_24 hpi and/or AOI_48 hpi plants (e.g. 'AO_24 hpi/AOC' and/or 'AO_48 hpi/AOC' comparisons) (Table S4), compared with respective non-infected control, were selected as core genes that might play an important role in the resistance of wild AK to *P. asparagi* (Fig. 3C; Table S7). Genotype-genotype correlation analysis based on these core DEGs also showed high correlations between AOI_24 hpi and AOI_48 hpi (r = 0.76), and between AKI_24 hpi and AKI_48 hpi (r = 0.70), but very low correlations between AKI_24 hpi and AOI_24 hpi (r = 0.03), and between 'AKI_48 hpi and AOI_48 hpi' (r = -0.07) (Fig. 3D).

Functional enrichment and RT-qPCR analyses of DEGs

The selected 211 core DEGs were subjected to an enrichment analysis using Kyoto Encyclopedia of Genes and Genomes (KEGG) database to assess their potential metabolic regulatory roles. Results showed 11 significantly ($P < 0.05$) enriched pathways, including primary metabolite metabolism ['tyrosine metabolism (aof00350)' and 'tryptophan metabolism (aof00380)'], secondary metabolite biosynthesis ['phenylalanine metabolism (aof00360)', 'flavonoid biosynthesis (aof00941)' and 'isoquinoline alkaloid biosynthesis

(aof00950)'], plant defense signaling and transcript regulation ['plant-pathogen interaction (aof04626)', 'protein processing in endoplasmic reticulum (aof04141)', 'protein export (aof03060)', 'plant hormone signal transduction (aof04075') and 'spliceosome (aof03040)'], and 'circadian rhythm (aof04712)' (Fig. 4A). We then conducted a gene-metabolite correlation analysis using the 211 core genes and metabolite data matrix in the examined AK plants (Fig. 4B). Results revealed a strong relationship between the 211 core genes and most of the metabolites, which showed upregulated expression and increased contents, respectively, in the resistant AK plants, indicating that these core genes and metabolites play essential roles in the defense responses of AK plants against *P. asparagi* (Fig. 4B). However, asparagusic acid glucose esters, which decreased in the resistant AK plants, showed negative correlation with the identified upregulated core genes (Fig. 4B). Real-time qPCR (RT-qPCR) was performed using 6 randomly selected genes from these 211 core genes and 4 from other DEGs to validate the RNA-seq data. The expression levels of these tested genes obtained by RT-qPCR and RNA-seq were comparable, strengthening the reliability of the transcriptome data analyzed using the latest transcript version Aspof.V1 (Fig. 5A-B).

Distribution and verification of SNP and Indel markers in susceptible *A. officinalis* and resistant wild *A. kiusianus*

In total, 204,756 and 580,110 high-quality SNPs, and 119,767 and 154,059 high-quality Indels were found in the AO and AK transcriptomes, respectively (Fig. 6A-C). Of these, 56,685 SNPs and 48,528 Indels were overlapping between susceptible AO and resistant AK plants (Fig. 6A). The frequencies of transition-type SNPs detected in AO and AK were 60.71 and 63.23%, respectively, which were higher than that of the transversion-type SNPs (39.28 and 36.76%, respectively) (Fig. 6B). The transition-type SNP frequencies for A-to-G nucleotides (62,681 and 183,838) and C-to-T nucleotides (61,644 and 183,005, respectively) were very much different in AO and AK plants. Similarly, the frequencies of the four transversion-type SNPs (A-to-C, A-to-T, G-to-C and G-to-T) were also different in both species (Fig. 6B). The ratios of SNP transitions/transversions were 1.54 and 1.72 in AO and AK, respectively (Fig. 6B). Regarding Indel distributions, the ratios of deletions and insertions of 'A and/or T' relative to 'G and/or C' base pairs were 8.02 and 1.12 in AO and AK plants, respectively (Fig. 6C).

Based on the obtained data, 12 simple sequence repeat (SSR), cleaved amplified polymorphic sequence (CAPS) and Indel markers were designed and tested for their usefulness in discriminating AO and AK species using the genomic DNA samples extracted

from four AO accessions (AO0012M, AO0606F, Glm002H and WC9), four AK accessions (AK0101M, AK0301, AK0401 and AK0501), and an F_1 hybrid between AO × AK (Fig. 7A-C; Table S8). All the 12 markers exhibited polymorphic patterns between the AO and AK accessions, which indicated their reliability for mapping of resistance traits (Fig. 7A-C).

Discussion

Our recent studies (Abdelrahman et al. 2017b; Takeuchi et al. 2017) showed that AK, a wild relative of cultivated AO, displayed much lower disease symptoms than the AO upon artificial inoculation with *P. asparagi*, suggesting that wild *Asparagus* species could act as potential genetic resources for generating novel asparagus cultivars with stem blight disease resistance through molecular breeding. In this study, the metabolome analysis of resistant wild AKI_24 hpi and AKI_48 hpi with *P. asparagi* using LC-Q-TOF-MS and MS/MS showed a rapid increase in several flavonoids and steroidal saponins, including anthocyanins [cyanidin-hex-dhex-hex (C1), cyanidin 3-rutinosides (C4 and C6) and idaein/cyanidin 3-O-galactosides (C7 and C8)], flavone [5,6,7,4'-tetrahydroxy-8-methoxyisoflavone-hex (C12)] and steroidal saponins [protodiosin (C9) and furost-ene-triol-hex-dhex-hex (C13)], but a decrease in asparagusic acid glucose esters (C2 and C3) in comparison with non-inoculated AKC plants (Figs. 1A-B and 2C-D; Table S3). On the other hand, no DPMs were detected in the susceptible AOI_24 hpi and AOI_48 hpi relative to non-inoculated AOC plants (Fig. 2C-D; Table S3). The metabolome data indicated a rapid metabolic change toward the accumulations of anthocyanin and saponin defense-related metabolites in resistant wild AK in comparison with susceptible AO plants, which could contribute to the stem blight disease resistance phenotype in the AK species. Cultivated *Asparagus* species are highly packed with essential vitamins and minerals, in addition to functional compounds like flavonoids, saponins and sulfur-containing ones that possess strong antioxidant and antimicrobial properties (Sakaguchi et al. 2008; Di Maro et al. 2013, Jaramillo-Carmona et al. 2017; Chitrakar et al. 2019; Dong et al. 2019). However, wild *Asparagus* species, such as *A. pseudoscaber*, *A. maritimus*, *A. brachiphyllus* and *A. prostrates*, have been reported to possess higher levels of protodioscin-type (e.g. steroidal saponins), and the total saponin levels were found to be ~10-fold higher in wild *Asparagus* species than in commercial *A. officinalis* cultivars (Jaramillo-Carmona et al. 2017). Fifteen types of anthocyanins (cyanidin and peonidin and their glucoside derivatives) have been identified in different purple and green asparagus cultivars (Dong et al. 2019). However, the ratios of anthocyanin compounds

varied in different *Asparagus* species and *A. officinalis* (Sakaguchi et al. 2008). Anthocyanins and saponins are well known defense-related metabolites that play major roles in plant protection against pathogens (Mostafa et al. 2013; Abdelrahman et al. 2015; Lu et al. 2017; Abdelrahman et al., 2017c; Abdelrahman et al. 2019a; Hussain et al. 2019). For instance, an early study by He et al. (2001) demonstrated that the activation of phenylammonia lyase, an upstream enzyme in the flavonol and anthocyanin biosynthesis pathway, induced the resistance of *A. densiflorus* against *Fusarium oxysporum* f.sp. *asparagi*. Likewise, several saponin compounds with potent antifungal and cytotoxic properties have been isolated from wild *Asparagus* species (Jaramillo-Carmona et al. 2017; Srivastava et al. 2018). Thus, our results along with published reports suggested that increasing the levels of anthocyanin glucosides and saponins might be an effective strategy to enhance the resistance of asparagus cultivars against *P. asparagi*.

To identify genes that involved in *Phomopsis* disease resistance, and the correlations between the gene expression and metabolic changes, we conducted a pairwise analysis comparing the transcriptome changes in four comparisons, namely 'AKI_24 hpi/AKC', 'AKI_48/AKC', 'AKI_24 hpi/AOI_24 hpi' and 'AKI_48 hpi/AOI_48 hpi' (Fig. 3A-C). In total, 211 genes were identified as the core gene set that exhibited upregulation in 'AKI_24 hpi/AKC' and/or 'AKI_48/AKC' comparisons, but downregulated in 'AOI_24 hpi/AOC' and/or 'AOI_48 hpi/AOC' comparisons (Fig. 3A-C; Tables S4, S5 and S7). KEGG enrichment analysis of these 211 core genes demonstrated significant enrichment in various known resistance-relevant metabolic and signaling pathways, such as 'flavonoid biosynthesis, 'plant-pathogen interaction', 'plant hormone signal transduction', 'protein processing in endoplasmic reticulum', and some others (Fig. 4A). Among these 211 core genes, *chalcone--flavonone isomerase 3* (*CHI3*), *flavonoid 3'-monooxygenase-like* (*F3'H-L*)/*CYP75B1*, *UV resistance locus 8-like* (*UVR8-L*) and *repressor of UV-B photomorphogenesis-like* (*RUP2-L*) genes were upregulated in the resistant AKI_24 and 48 hpi versus susceptible AOI_24 and 48 hpi, respectively (e.g. 'AKI_24 hpi/AOI_24 hpi' and/or 'AKI_48 hpi/AOI_48 hpi' comparisons) (Tables S6 and S7). CHI enzyme catalyzes the cyclization of chalcones into naringenin, while F3'H catalyzes the conversation of naringenin into eriodictyol, and then dihydrokaempferol into dihydroquercetin that is an important precursor for anthocyanin biosynthesis (Olsen et al. 2010; Ferreyra et al. 2012). Similarly, *UVR8-L* gene, which is induced not only by UV-B irradiation but also by other stresses, has an important role in the accumulation of anthocyanins in plants through its interaction with members of the WD40-repeat protein family, such as RUP1 and RUP2 that are involved in regulation of anthocyanin

biosynthesis (Tossi et al. 2019). With respect to steroidal saponins, *Δ(24)-sterol reductase-like* (*DHCR24-L*) and *sterol 3-β-glucosyltransferase* (*SGT1*) genes that are involved in the downstream processes of steroidal saponin biosynthesis were upregulated in 'AKI_24 hpi/AOI_24 hpi' and/or 'AKI_48 hpi/AOI_48 hpi' comparisons (Tables S6 and S7). Silencing of *Withania somnifera SGT* gene changed the steroidal saponin ratio by decreasing withanoside V level and increasing the contents of withanolide A, sitosterol and stigmasterol, resulting in high susceptibility to *Alternaria alternata* infection (Singh et al. 2016). In summary, results of this study revealed that the changes in gene expression were correlated with the changes in metabolic profiles, specifically with respect to the accumulations of anthocyanins and steroidal saponins in AK species. Further studies are required to examine the functions of the identified genes related to the biosyntheses of anthocyanins and steroidal saponins in *Asparagus* defense against *P. asparagi.*

In addition to gene-metabolite correlation results, KEGG enrichment analysis of the 211 core genes demonstrated an enrichment in 'plant-pathogen interaction' and 'protein processing in endoplasmic reticulum' pathways (Fig. 4A). For example, genes implicated in pathogen recognition and induction of plant defense responses, such as *subtilisin-like protease 1* (*SBT1*), *S-norcoclaurine synthase 1* (*NCS1*/*PR10*), *peroxidase 29* (*POX29*), *catalase isozyme 1-like* (*CAT1-L*), *glutathione S-transferase* (*GST*), *salicylic acid-binding protein 2* (*SABP2*) and *2-oxoisovalerate dehydrogenase subunit alpha 2* (*BCKDHA2*), were exclusively upregulated in resistant AK_24 and/or 48 hpi (e.g. 'AKI_24 hpi/AKC' and/or 'AKI_48/AKC' comparisons) and downregulated in susceptible AOI_24 and/or AOI_48 hpi, compared with uninfected control (e.g. 'AO_24 hpi/AOC' and/or 'AO_48 hpi/AOC' comparisons) (Fig. 5; Tables S4, S5 and S7). Monteiro et al. (2013) showed the importance of *SBT* upregulation in the resistance of the resistant grapevine (*Vitis vinifera*) genotypes to *Plasmopara viticola* infection, when compared with the susceptible ones. In addition, overexpression of *Arabidopsis SBT3.3* promoted chromatin remodeling and activated immune response through salicylic acid-dependent mechanisms against *P. syringae* infection as compared with *Arabidopsis sbt3.3* mutant plants, indicating that SBT is important for induction of early hypersensitive immune responses in plants (Ramírez et al. 2013). Similarly, POX and CAT are well known antioxidant enzymes that play potential roles in plant signaling and/or in oxidative stress resistance associated with resistant genotypes relative to susceptible ones (Taggar et al. 2012; Nowogórska and Patykowski 2015).

In addition, we also successfully identified in this study some important resistance-related candidate genes, the so-called *R* genes like *leucine rich repeat receptor-like*

serine/*threonine-protein kinase* (*LRR-RLPK*), *LRR-RLPK-barely any meristem 1* (*LRR-RLPK-BAM1*) and *probable serine*/*threonine protein kinase* (*PK-IRE4*) (Table S7). These *R* genes are very useful candidates that can be used for molecular breeding to induce disease resistance in susceptible cultivars (Ashkani et al. 2015; Garrett et al. 2017). Furthermore, our data demonstrated that several inositol biosynthesis- and transport-related genes, including *inositol-3-phosphate synthase* (*IPS*), *inositol transporter 1* (*INT1*), *inositol-tetrakisphosphate 1-kinase 3-like* (*ITPK3-L*) and *inositol hexakisphosphate and diphosphoinositol-pentakisphosphate kinase 2* (*PPIP5K2*), were enriched in the upregulated gene sets of resistant wild AKI_24 and/or 48 hpi and downregulated in susceptible AOI_24 and/or 48 hpi, compared with uninfected control (Table S4, S5 and S7). RNA-seq profiling of the defense-associated transcriptomes of *Brachypodium distachyon* and wheat (*Triticum aestivum*) during infection with *F. pseudograminearum* showed upregulation in *INT* and *GST* genes, suggesting that these genes might have significant roles in cereal defenses against fungal infection (Powell et al. 2017). In addition, *Arabidopsis ips2* mutant plants exhibited lower levels of *myo*-inositol hexakisphosphate and displayed higher susceptibility to cucumber (*Cucumis sativus*) mosaic virus, *Botrytis cinerea* and *P. syringae* infections than wild-type plants (Murphy et al. 2008). Our results and these published reports collectively suggested that inositol biosynthesis- and transport-related genes might play important roles in the AK defenses against *P. asparagi*. Detailed genetic studies using overexpression and/or mutations of *IPS*, *INT* and/or *IPTK* genes might provide a confirmatory picture for their *in planta* functions in asparagus, as well as a new avenue for inducing defense mechanisms through inositol biosynthesis and signaling pathways.

In addition, the comparative analysis of the AO and AK transcriptomes also revealed a great number of high-quality SNPs and Indels. These data enabled us to develop various Indel, SSR and CAPS markers that indeed exhibited polymorphic patterns, suggesting their usefulness for generation of a high-density linkage map to facilitate the applications of molecular marker-assisted selection for development of *A. officinalis* cultivars with improved *P. asparagi* resistance (Fig. 7).

Conclusions

In this study, the comprehensive metabolome and transcriptome analyses of susceptible AO and resistant wild AK plants 24 and 48 hpi with *P. asparagi* revealed a good correlation of accumulated anthocyanins and steroidal saponins with defense against stem blight disease. In addition, we identified 211 core genes that were exclusively upregulated in resistant wild AK

and downregulated in susceptible AO plants. These core genes might have important roles in several metabolic and plant-signaling defense pathways, contributing to the stem blight disease-resistant phenotype of the AK species. Furthermore, the generation of a high-quality set of SNPs and Indels using the AO and AK transcriptome data enabled us to develop various Indel, SSR and CAPS markers for future development of a high-density linkage map that could be used for selection of improved stem blight disease-resistant *Asparagus* cultivars.

Methods

Plant materials and sampling

Female *Phomopsis*-susceptible *A. officinalis* cultivar 'Mary Washington 500W' (AO0060 strain) and male *Phomopsis*-resistant wild *A. kiusianus* (AK0501 strain) (Abdelrahman et al. 2017b) plant species were cultivated for 5 years at Kagawa prefectural agricultural experiment station (Kagawa, Japan). A commercial soil consisting of well-drained clay, loam, leaf mold and garden soil (2:1:1:4 and 2:1:1:2 v:v ratios for *A. officinalis* and *A. kiusianus*, respectively), which was supplied with 500 mg P kg^{-1}, 50 mg N kg^{-1} and 100 mg K kg^{-1} [water holding capacity of ~70%; pH 6–6.5; Nippi Engei Baido No.1 (Nihon Hiryo Co. Ltd.)] as a root-supporting medium, was used for growing plants.

Asparagus species were artificially inoculated with spore suspension of *P. asparagi* at a final concentration of 10^7 CFU mL^{-1} using the vinyl cotton method (Sonoda et al. 1997), with some modifications: water-retentive polyester fiber sheeting was used instead of cotton, and silicone tubes were used rather than vinyl tubes. Stems from three independent biological replicates (n = 3) were harvested 24 and 48 hpi with *P. asparagi*, immediately frozen in liquid nitrogen, and stored at −80°C until further processing. Non-inoculated *Asparagus* plants grown under the same conditions served as controls.

Four AO accessions [(AO0012M (male), AO0606F (female), Glm002H (male) and WC9 (female)] and four *A. kiusianus* accessions [AK0101M (male), AK0301 (female), AK0401 (male) and AK0501 (male)] were used for analysis of InDel, SSR and CAPS markers. AO0012M, AO0606F, Glm002H and WC9 accessions were derived from 'Mary Washington 500W', 'Pacific 2000', 'Gijnlim' and 'UC157F1' cultivars, respectively. AK0101M, AK0301 and AK0401 accessions were wild individuals collected from different locations.

Metabolome analysis

Stem samples collected from AO and AK plants with or without inoculation with *P. asparagi* [two *Asparagus* species × three biological replicates × three treatments (control, 24 hpi and 48 hpi), a total of 18 samples] were subjected to an extraction with 5 μL (per mg fresh weight of sample) of 80% MeOH solution, which contained 2.5 μM lidocaine and 10-camphour sulfonic acid, using a mixer mill with zirconia beads for 7 min at 18 Hz and 4°C (Tsugawa et al. 2019). After centrifugation for 10 min at 17000 g and 4°C, the supernatant was filtered using an HLB μElution plate (Waters, USA). The extracts (1.0 μL per sample) were analyzed using LC-Q-TOF-MS (LC, Waters Acquity UPLC system; MS, Waters Xevo G2 Q-Tof). MS/MS data were acquired in the ramp mode. All LC-Q-TOF-MS and MS/MS conditions are summarized in Table S9. Peaks with intensity greater than 2000 (noise level) were recorded. A peak of intensity less than 2000 was transposed to an intensity of 2000 so that it is not be subjected to the influence of noise. The KNApSAck software (Nakamura et al. 2014), Dictionary of Natural Products (http://dnp.chemnetbase.com/faces/chemical/ChemicalSearch.xhtml) and *Asparagus* saponin-related reports (Zhang et al. 2004; Hayes et al. 2008; Sharma et al. 2009; Shen et al. 2011; Dawid and Hofmann 2012; Vázquez-Castilla et al. 2013) were used for metabolite annotation. The intensity values of the peaks were divided by those of lidocaine for normalization. DPMs were identified using Student's *t*-test ($P < 0.05$) and FC ($FC \geq 2.0$ or $FC \leq 0.5$) as minimum cutoffs. PCA, boxplots, correlations and heatmaps were generated by the R v 3.5.1 (https://www.r-project.org). Metabolite network was generated by using Cystoscape v.3.5.1 (https://cytoscape.org) according to Abdelrahman et al. (2019a).

Data filtering, transcriptome assembly and DEG analysis

Clean reads were obtained from 18 stem samples collected from AO and AK plants after RNA-seq and filtering as described in Abdelrahman et al. (2018). The high-quality reads were mapped to the AO transcript reference (Aspof. V1) (Harkess et al. 2017) using Bowtie2 (Langmead and Salzberg 2012). The relative abundance of each transcript/isoform was calculated using RSEM v1.2.15 (Li and Dewey 2011), and Trimmed Mean of M-values (TMM) was used to normalize gene expression (Robinson and Oshlack 2010). DEGs were identified using edgeR (Robinson et al. 2010), and FDR and FC ($FC \geq 2.0$ or $FC \leq 0.5$; $FDR < 0.05$) were used as minimum cutoffs. KEGG enrichment analysis of core genes was carried out using the 'clusterProfiler' package in R v.3.5.1 (https://www.r-project.org).

Validation of RNA-seq data by RT-qPCR

Gene-specific primers and standard internal primers were designed using the aligned sequences of AO and AK cDNAs obtained from the Illumina RNA-seq data. RT-qPCR was performed using a SYBR Green Supermix Kit (Bio-Rad Laboratories, Inc.) and a Mini Option Real-Time PCR system (Bio-Rad). The specificity of all amplifications was confirmed by single-peak melting curves (Abdelrahman et al., 2017b). Relative expression levels were calculated using the ($2^{-\Delta C_T}$) method, with *elongation factor* (*EF*) gene as an internal standard. All reactions were performed with three biological replicates ($n = 3$), and means and standard deviations (SDs) of three biological replicates were calculated. Primers used in the RT-qPCR are listed in Table S8.

Identification and validation of genic-InDels and -SNPs

SNP and InDel data were downloaded from Abdelrahman et al. (2018) for analysis. CAPS, SSR and InDel-primer pairs (Table S8) were developed using Primer3 (http://bioinfo.ut.ee/primer3-0.4.0/), and were used to screen the AO (AO0012M, AO0606F, Glm002H and WC9) and AK (AK0101M, AK0301, AK0401 and AK0501) accessions, and an F_1 hybrid generated by a cross of AO 'Mary Washington 500W' cultivar and AK AK0501 accession. Genomic DNA samples used in the assay were extracted from the plants with the aid of the MagExtractor Plant Genome kit (TOYOBO Co., LTD., Osaka, Japan).

Availability of data

All raw fastq data are available in the SRA NCBI repository accession PRJNA435656, gene expression omnibus (GEO) NCBI accession GSE141012 and Kazusa Institute (ftp.kazusa.or.jp).

Funding

This work was supported by a Grant-in-Aid from the Ministry of Agriculture, Forestry and Fisheries (MAFF) (Japan) in the Science and Technology Research Promotion Program for Agriculture, Forestry, Fisheries, and Food industry. Mostafa Abdelrahman was supported by a fellowship from the Japan Society for the Promotion of Science ID P18080.

Consent for publication

Not applicable.

Competing interests

The authors declare that they have no competing interests

Authors' contributions

MA and AK conceived the study. TI, MM, KM, YO, MM, AU and AK performed plant inoculation and sample collection. MA performed RNA extractions and RNA-seq data analysis with the input of L-SPT. MA, RN and TM performed metabolome analysis. MA, HT, L-SPT and AK contributed to the writing of the initial draft of the manuscript. All authors read and approved the final manuscript.

References

Abdelrahman, M., Burritt, D.J., Gupta, A., Tsujimoto, h., Tran, L.P. (2019b) Heat stress effects on source-sink relationships and metabolome dynamics in wheat. *Experimental Botany* 71: 543–554

Abdelrahman, M., El-Sayed, M., Sato, S., Hirakawa, H., Ito, S.I., Tanaka, K., et al. (2017c) RNA-sequencing-based transcriptome and biochemical analyses of steroidal saponin pathway in a complete set of *Allium fistulosum-A. cepa* monosomic addition lines. *PLoS One* 12: e0181784.

Abdelrahman, M., Hirata, S., Sawada, Y., Hirai, M.Y., Sato, S., Hirakawa, H., et al. (2019a) Widely targeted metabolome and transcriptome landscapes of *Allium fistulosum–A. cepa* chromosome addition lines revealed a flavonoid hot spot on chromosome 5A. *Scientific Reports* 9: 3541.

Abdelrahman, M., Jogaiah, S., Burritt, D.J., Tran, L.P. (2018) Legume genetic resources and transcriptome dynamics under abiotic stress conditions. Plant Cell Environ. doi: 10.1111/pce.13123.

Abdelrahman, M., Mitoma, M., Ikeuchi, T., Mori, M., Murakami, K.,Ozakid, Y. (2018) Differential gene expression analysis and SNP/InDel marker discovery in resistant wild *Asparagus kiusianus* and susceptible *A. officinalis* in response to *Phomopsis asparagi* infection. *Data in Brief* 21: 2117–2121.

Abdelrahman, M., Sawada, Y., Nakabayashi, R., Sato, S., Hirakawa, H., El-Sayed, M., et al. (2015) Integrating transcriptome and target metabolome variability in doubled haploids of *Allium cepa* for abiotic stress protection. *Molecular Breeding* 35: 195.

Abdelrahman, M., Suzumura, N., Mitoma, M., Matsuo, S., Ikeuchi, T., Mori, M., et al. (2017b) Comparative *de novo* transcriptome profiles in *Asparagus officinalis* and *A. kiusianus* during the early stage of *Phomopsis asparagi* infection. *Scientific Reports* 7: 2608.

Ashkani, S., Rafii, M.Y., Shabanimofrad, M., Miah, G., Sahebi, M., Azizi, P., et al. (2015) Molecular breeding strategy and challenges towards improvement of blast disease resistance in rice crop. *Front Plant Science* 6: 886.

Cheah, L-H., Horlock, C.M. (2007) Field-applied fungicides and postharvest treatments to control *Asparagus* diseases posing biosecurity threats to New Zealand. New Zealand. *Plant Protection* 60:94–98.

Chitrakar, B., Zhang, M., Adhikari, B. (2019) Asparagus (*Asparagus officinalis*): Processing effect on nutritional and phytochemical composition of spear and hard-stem byproducts. *Trends Food Science Technology* 93: 1–11.

Dawid, C., Hofmann, T. (2012) Identification of sensory-active phytochemicals in *Asparagus* (*Asparagus officinalis* L.). *J Agriculture Food Chemistry* 60: 11877–11888.

Di Maro, A., Pacifico, S., Fiorentino, A., Galasso, S., Gallicchio, M., Guida, V., et al. (2013) Raviscanina wild asparagus (*Asparagus acutifolius* L.): A nutritionally valuable crop with antioxidant and antiproliferative properties. *Food Research International* 53:180–188.

Die, J.V., Castro, P., Millán, T., Gil, J. (2018) Segmental and tandem duplications driving the recent *NBS-LRR* gene expansion in the *Asparagus* genome. *Genes* 9: 568.

Dong, T., Han, R., Yu, J., Zhu, M., Zhang, Y., Gong, Y., Li, Z. (2019) Anthocyanins accumulation and molecular analysis of correlated genes by metabolome and transcriptome in green and purple asparaguses (*Asparagus officinalis*, L.). *Food Chemistry* 217: 18–28.

Ferreyra, M.L.F., Rius, S.P., Casati, P. (2012) Flavonoids: biosynthesis, biological functions, and biotechnological applications. *Frontiers Plant Science* 3: 222.

Garrett, A.K., Andersen, K.F., Asche, F., Bowden, R.L., Forbes, G.A., Kulakow, P.A., et al. (2017) Resistance genes in global crop breeding networks. *Phytopathology* 107: 1268-1278.

Harkess, A., Zhou, J., Xu, C., Bowers, J.E., Van der Hulst, R., Ayyampalayam, S., et al. (2017) Origin and evolution of a young Y chromosome. *Nature Communications* 8:1279.

Hayes, P.Y., Jahidin, A.H., Lehmann, R., Penman, K., Kitching, W., De Voss, J.J. (2008) Steroidal saponins from the roots of *Asparagus racemosus*. *Phytochemistry* 69: 796-804.

He, C., Hsiang, T., Wolyn, D.J. (2001) Activation of defense responses to *Fusarium* infection in *Asparagus densiflorus*. *European J Plant Pathology* 107: 473–483.

Hussain, M., Debnath, B., Qasim, M., Bamisile, B.S., Islam, W., Hameed, M.S., et al. (2019) Role of saponins in plant defense against specialist herbivores. *Molecules* 24: 2067.

Ito, T., Konno, I., Kubota, S., Ochiai, T., Sonoda, T., Hayashi, Y., et al. (2011) Production and characterization of interspecific hybrids between *Asparagus kiusianus* Makino and *A. officinalis* L. *Euphytica* 182: 285–294.

Iwato, M., Kosaza, M., Takeuchi, Y., Matsumoto, M., Inada, M., Ozaki, Y., et al. (2014) Stem blight resistance of *Asparagus kiusianus* and its hybrid with *A. officinalis*. *Advances Horticultural Science* 28: 202–207.

Jaramillo-Carmona, S., Rodriguez-Arcos, R, Jiménez-Araujo, A., López, S., Gil, J., Moreno, R., Guillén-Bejarano, R. (2017) Saponin profile of wild *Asparagus* species. *Food Science* 82: 638–646.

Kim, D., Pertea, G., Trapnell, C., Pimentel, H., Kelley, R., Salzberg, S.L. (2013) TopHat2: accurate alignment of transcriptomes in the presence of insertions, deletions and gene fusions. *Genome Biology* 14: R36.

Kubota, S., Konno, I., Kanno, K. (2012) Molecular phylogeny of the genus *Asparagus* (Asparagaceae) explains interspecific crossability between the garden asparagus (*A. officinalis*) and other *Asparagus* species. *Theoretical Applied Genetics* 124:345–354.

Langmead, B., Salzberg, S.L. (2012) Fast gapped-read alignment with Bowtie 2. *Nature Methods* 9: 357–359.

Lei, Z., Zhou, C., Ji, X., Wei, G., Huang, Y., Yu, W., et al. (2018) Transcriptome analysis reveals genes involved in flavonoid biosynthesis and accumulation in *Dendrobium catenatum* from different locations. *Scientific Reports* 8: 6373.

Li, B., Dewey, C.N. (2011) RSEM: accurate transcript quantification from RNA-Seq data with or without a reference genome. *BMC Bioinformatics* 12:323.

Lu, Y., Chen, Q., Bu, Y., Luo, R., Hao, S., Zhang, J., et al. (2017) Flavonoid accumulation plays an important role in the rust resistance of malus plant leaves. *Frontiers Plant Science* 8: 1286.

Matsuda, F., Nakabayashi, R., Yang, Z., Okazaki, Y., Yonemaru, J-I., Ebana, K., et al. (2015) Metabolome-genome-wide association study dissects genetic architecture for generating natural variation in rice secondary metabolism. *Plant J* 81: 13-23.

Monteiro, F., Sebastiana, M., Pais, M., Figueiredo, A. (2013) Reference gene selection and validation for the early responses to downy mildew infection in susceptible and resistant *Vitis vinifera* cultivars. *PLoS ONE* 8:e72998.

Mostafa, A., Sudisha, J., El-Sayed, M., Ito, S., Ikeda, T., Yamauchi, N., et al. (2013) Aginoside saponin, a potent antifungal compound, and secondary metabolite analyses from *Allium nigrum* L. *Phytochem Lett* 6: 274–280.

Murphy, A.M., Otto, B., Brearley, C.A., Carr, J.P., Hanke, D.E. (2008) A role for inositol hexakisphosphate in the maintenance of basal resistance to plant pathogens. *Plant J* 56: 638–652.

Nakamura, Y., Afendi, F.M., Parvin, A.K., Ono, N., Tanaka, K., Hirai Morita, A., et al. (2014) KNApSAcK Metabolite Activity Database for retrieving the relationships between metabolites and biological activities. *Plant Cell Physiology* 55:e7.

Negi, J.S., Singh, P., Joshi, G.P., Rawat, M.S., Bisht, V.K. (2010) Chemical constituents of *Asparagus*. *Pharmacogn Rev* 4: 215–220.

Nowogórska, A., Patykowski, J. (2015) Selected reactive oxygen species and antioxidant enzymes in common bean after *Pseudomonas syringae* pv. *phaseolicola* and *Botrytis cinerea* infection. *Acta Physiologiae Plantarum* 37:1725.

Olsen, K.M., Hehn, A., Jugdé, H., Slimestad, R., Larbat, R., Bourgaud, F. (2010) Identification and characterisation of CYP75A31, a new flavonoid 3'5'-hydroxylase, isolated from *Solanum lycopersicum*. *BMC Plant Biology* 10: 21.

Powell, J.J., Carere, J., Sablok, G., Fitzgerald, T.L., Stiller, J., Colgrave, M.L., et al. (2017) Transcriptome analysis of *Brachypodium* during fungal pathogen infection reveals both shared and distinct defense responses with wheat. *Scientific Reports* 7:17212.

Ramírez, V., López, A., Mauch-Mani, B., José Gil, M., Vera, P. (2013) An extracellular subtilase switch for immune priming in *Arabidopsis*. *PLOS Pathogens* 12: e1006003.

Robinson, M.D., McCarthy, D.J., Smyth, G.K. (2010) edgeR: a Bioconductor package for differential expression analysis of digital gene expression data. *Bioinformatics* 26: 139–140.

Robinson, M.D., Oshlack, A. (2010) A scaling normalization method for differential expression analysis of RNA-seq data. *Genome Biology* 11: R25.

Roos, J., Hopkins, R., Kvarnheden, A., Dixelius, C. (2011) The impact of global warming on plant diseases and insect vectors in Sweden. *European J Plant Patholo*gy 129: 9–19.

Sakaguchi, Y., Mine, Y., Okubo, H. and Ozaki, Y. (2008). Anthocyanin variation in *Asparagus* species and its inheritance *Acta Horticulturae* 776: 285–290.

Sharma, U., Saini, R., Bobita, Kumar, N., Singh, B. (2009). Steroidal saponins from *Asparagus racemosus*. *Chemical Pharmaceutical Bulletin* 57: 890–893.

Singh, G., Tiwari, M., Singh, S.P., Singh, S., Trivedi, P.K., Misra, P. (2016) Silencing of sterol glycosyltransferases modulates the withanolide biosynthesis and leads to compromised basal immunity of *Withania somnifera*. *Scientific Reports* 6: 25562.

Shen, Y., Xu, C-L., Xuan, W-D., Li, H-L., Liu, R-H., Xu, X-K., Chen H-S. (2011) A new furostanol saponin from *Asparagus cochinchinensis*. *Archives Pharmacal Research* 34: 1587–1591.

Sonoda, T., Uragami, A., Itoh, K., Kohmura, H., Ohwada, M., Kaji, K. (2001) Evaluation of *Asparagus* species and comparison between sexes in *A. officinalis* cultivars for resistance to stem blight. *J Japanese Society Horticultural Science* 70:244–250.

Sonoda, T., Uragami, A., Kaji, K. (1997) Evaluation of *Asparagus officinalis* cultivars for resistance to stem blight by using a novel inoculation method. *Horticultural Science* 32:1085–1086.

Srivastava, P.L., Shukla, S., Kalunke, R.M. (2018) Comprehensive metabolic and transcriptomic profiling of various tissues provide insights for saponin biosynthesis in the medicinally important *Asparagus racemosus*. *Scientific Reports* 8: 9098.

Taggar, G.K., Gill, R.S., Gupta, A.K., Sandhu, J.S. (2012) Fluctuations in peroxidase and catalase activities of resistant and susceptible black gram (*Vigna mungo* (L.) Hepper) genotypes elicited by *Bemisia tabaci* (Gennadius) feeding. *Plant Signaling Behavior* 7: 1321–1329.

Takahashi, H., Yoshida, C., Takeda, T. (2019) Sugar composition in *Asparagus* spears and its relationship to soil chemical properties. *Journal Applied Glycoscience* 66: 47–50.

Takeuchi, Y., Kakizoe, E., Yoritomi, R., Iwato, M., Kanno, A., Ikeuchi, T., et al. (2017) Features in stem blight resistance confirmed in interspecific hybrids of *Asparagus officinalis* L. and *Asparagus kiusianus* Makino. *Horticult J* 87: 200–205.

Thao, L.D., Dung, N.T. (2019) First report of *Phomopsis asparagi* causing stem blight on asparagus in Vietnam. *New Disease Reports* 39: 7.

Tossi, V.E., Regalado, J.J., Iannicelli, J., Laino, L.E., Burrieza, H.P., Escandón, A.S., et al. (2019) Beyond *Arabidopsis*: Differential UV-B response mediated by UVR8 in diverse species. *Frontiers Plant Science* 10: 780.

Tsugawa, H., Nakabayashi, R., Mori, T., Yamada, Y., Takahashi, M., Rai, A., et al. (2019) A cheminformatics approach to characterize metabolomes in stable-isotope-labeled organisms. *Nature Methods* 16: 295–298.

Vázquez-Castilla, S., Jaramillo-Carmona, S., Fuentes-Alventosa, J.M., Jiménez-Araujo, A., Rodriguez-Arcos, R., Cermeño-Sacristán, P., et al. (2013) Optimization of a method for the profiling and quantification of saponins in different green asparagus genotypes. *J Agriculture Food Chemistry* 61: 6250-6258.Xiao, J.F., Zhou, B., Ressom, H.W. (2012) Metabolite identification and quantitation in LC-MS/MS-based metabolomics. *Trends Analytical Chemistry* 32: 1–14.

Yang, Y-Q., Lan, B., Jian, Y-L., Chang, D-D., Zhang, S-L., Li, X-M. (2016) Infection process and pathogenic mechanism of *Phomopsis asparagi*, the *Asparagus* stem blight pathogen. Phytoparasitica 44:11–18.

Yano, R., Takagi, K., Takada, Y., Mukaiyama, K., Tsukamoto, C., Sayama, T., et al. (2016) Metabolic switching of astringent and beneficial triterpenoid saponins in soybean is achieved by a loss-of-function mutation in cytochrome P450 72A69. *Plant J* 89: 527-539.

Yi, T.G., Yeoung, Y.R., Choi, I.Y., Park, N.I. (2019) Transcriptome analysis of *Asparagus officinalis* reveals genes involved in the biosynthesis of rutin and protodioscin. *PLoS One* 14: e0219973.

Zaw, M., Naing, T.A.A., Matsumoto, M., (2017) First report of stem blight of asparagus caused by *Phomopsis asparagi* in Myanmar. *New Disease Reports* 35: 17.

Zhang, H-J., Sydara, K., Tan, G., Ma, C., Southavong, B., Soejarto, D.D., et al. (2004) Bioactive Constituents from *Asparagus cochinchinensis*. *J Natural Product* 67: 194-200.

Zhang, N., Sun, Q., Li, H., Li, X., Cao, Y., Zhang, H., et al. (2016) Melatonin improved anthocyanin accumulation by regulating gene expressions and resulted in high reactive oxygen species scavenging capacity in cabbage. *Frontiers Plant Science* 7: 197.

Table 1. Mapping statistics of *Asparagus officinalis* and *A. kiusianus* 24 and 48 h post-inoculation with *Phomopsis asparagi* (AOI_24 h hpi, AOI_48 hpi, AKI_24 hpi and AKI_48 hpi), and non-inoculated controls (AOC and AKC).

Sample ID	Total read count	Unmapped reads	Unique mapped reads	Multi mapped reads	Overall mapping
AKC_1	11682062	4863081 (41.63%)	4757367 (40.72%)	2061614 (17.65%)	58.37%
AKC_2	12303039	3041774 (24.72%)	6121132 (49.75%)	3140133 (25.52%)	75.28%
AKC_3	11359220	2720290 (23.95%)	5805277 (51.11%)	2833653 (24.95%)	76.05%
AKI_24 hpi_1	13577152	3394164 (25.00%)	6829954 (50.30%)	3353034 (24.70%)	75.00%
AKI_24 hpi_2	12314913	3001362 (24.37%)	6197337 (50.32%)	3116214 (25.30%)	75.63%
AKI_24 hpi_3	13009478	3097480 (23.81%)	6492599 (49.91%)	3419399 (26.28%)	76.19%
AKI_48 hpi_1	12086160	3300029 (27.30%)	5913268 (48.93%)	2872863 (23.77%)	72.70%
AKI_48 hpi_2	13151943	3282775 (24.96%)	6573589 (49.98%)	3295579 (25.06%)	75.04%
AKI_48 hpi_3	12196294	3271205 (26.82%)	5920135 (48.54%)	3004954 (24.64%)	73.18%
AOC_1	11199822	2217563 (19.80%)	6009348 (53.66%)	2972911 (26.54%)	80.20%
AOC_2	12722337	2595148 (20.40%)	6751484 (53.07%)	3375705 (26.53%)	79.60%
AOC_3	12398105	2396258 (19.33%)	6684544 (53.92%)	3317303 (26.76%)	80.67%
AOI_24 hpi_1	13310449	2650303 (19.91%)	7005679 (52.63%)	3654467 (27.46%)	80.09%
AOI_24 hpi_2	11242858	2074504 (18.45%)	6306250 (56.09%)	2862104 (25.46%)	81.55%
AOI_24 hpi_3	12470966	2391986 (19.18%)	6751730 (54.14%)	3327250 (26.68%)	80.82%
AOI_48 hpi_1	12341570	2331782 (18.89%)	6637159 (53.78%)	3372629 (27.33%)	81.11%
AOI_48 hpi_2	11004652	2105468 (19.13%)	5851287 (53.17%)	3047897 (27.70%)	80.87%
AOI_48 hpi_3	10403106	2045084 (19.66%)	5497813 (52.85%)	2860209 (27.49%)	80.34%

Figure legends

Fig. 1 Principal component analysis (PCA) of the assigned metabolite signal intensities obtained from the susceptible cultivated *Asparagus officinalis* (AO) and resistant wild *A. kiusianus* (AK) plants 24 and 48 h post-inoculated with *Phomopsis asparagi* (AOI_24 hpi, AOI_48 hpi, AKI_24 hpi and AKI_48 hpi), and non-inoculated controls (AOC and AKC). (A-B) Score plots of metabolite signal intensities detected by using positive (A) and negative (B) ion modes of liquid chromatography-quadrupole time-of-flight mass spectrometry (LC-Q-TOF-MS).

Fig. 2 Metabolite profiles and correlation analyses of susceptible *Asparagus officinalis* (AO) and resistant wild *A. kiusianus* (AK) plants 24 and 48 h post-inoculated with *Phomopsis asparagi* (AOI_24 hpi, AOI_48 hpi, AKI_24 hpi and AKI_48 hpi), and non-inoculated controls (AOC and AKC). (A) Boxplot of the signal intensities of 14 metabolites identified in the examined *Asparagus* species. (B) Venn diagram of the 13 differentially produced metabolites in the examined *Asparagus* species in response to *P. asparagi*. Red and blue numbers indicated increased (FC $\geq$ 2.0; $P < 0.05$) and decreased (FC $\leq$ 0.5; $P < 0.05$) metabolites. (C) Heatmap hierarchal clustering of the 14 metabolite signal intensities in the investigated *Asparagus* species using the Z-scores. (D) Boxplots of cyanidin-hex-dhex-hex (C1), cyanidin 3-rutinoside (C4), idaein (C8), furost-ene-triol-hex-dhex-hex (C13) and asparagusic acid glucose ester (C2 and C3) signal intensities, which exhibited higher and lower accumulations, respectively, in the examined *Asparagus* species. (E) Metabolite-metabolite correlation network. (F) Genotype-genotype correlations of the examined *Asparagus* species. Significant letters indicate significant differences between examined *Asparagus* species in response to *P. asparagi* at $P < 0.05$, according to a Duncan multiple range test.

Fig. 3 Transcriptome profiles and correlation analyses of susceptible *Asparagus officinalis* (AO) and resistant wild *A. kiusianus* (AK) plants 24 and 48 h post-inoculated with *Phomopsis asparagi* (AOI_24 hpi, AOI_48 hpi, AKI_24 hpi and AKI_48 hpi), and non-inoculated controls (AOC and AKC). (A) Volcano plots of differentially expressed genes (DEGs) in the examined *Asparagus* species in response to *P. asparagi*. (B) Venn diagrams of overlapping

DEGs in examined *Asparagus* species in response to *P. asparagi*. (C) Heatmap hierarchical clustering of 211 core genes upregulated in resistant wild AKI-24 hpi and/or AKI_48 hpi versus non-treated control AKC, and downregulated in susceptible AOI_24 hpi and/or AOI_48 hpi versus non-treated control AOC. (D) Treatment and genotype-genotype correlations based on the Pearson correlation coefficient of the 211 core genes.

Fig. 4 Kyoto encyclopedia of genes and genomes (KEGG) enrichment analysis, and metabolite-gene correlation analysis. (A) KEGG enrichment analysis of 211 core genes that are upregulated in resistant wild *A. kiusianus* plants 24 and 48 h post-inoculated with *Phomopsis asparagi* (AKI_24 hpi and/or AKI_48 hpi) versus non-treated control AKC, and downregulated in susceptible *A. officinalis* (AOI_24 hpi and/or AOI_48 hpi) versus non-treated control AOC. (B) Correlation analysis of the 211 core genes and 13 differentially produced metabolites in the examined *Asparagus* species in response to *P. asparagi*.

Fig. 5 Expression patterns of 10 representative genes in *Asparagus officinalis* (AO) and *A. kiusianus* (AK) plants 24 and 48 h post-inoculated with *Phomopsis asparagi* (AOI_24 hpi, AOI_48 hpi, AKI_24 hpi, and AKI_48 hpi) and non-inoculated controls (AOC and AKC). (A) Expression levels were quantified by real-time quantitative PCR (RT-qPCR). (B) Fold changes in gene expression derived from the RNA-seq were used to generate the heatmap. Values represent the means of three independent biological replicates and standard deviations (n = 3). Different letters indicate significant differences among various treatments according to a Tukey's HSD.

Fig. 6 Single nucleotide polymorphism (SNP) and insertion/deletion (Indel) distributions in *Asparagus officinalis* and *A. kiusianus* transcriptome datasets. (A) Venn diagrams showing the distributions of overlapping SNPs and Indels in *A. officinalis* and *A. kiusianus* compared with the *A. officinalis* reference genome Aspof.V1. (B–C) Total number of transition-type and transversion-type SNPs (B), and Indel distribution (C) in *A. officinalis* and *A. kiusianus* transcriptomes. A_G, A-to-G; C_T, C-to-T; A_C, A-to-C; A_T, A-to-T; G_C, G-to-C; G_T, G-to-T.

Fig. 7 Verification and discrimination of examined *Asparagus* species using the designed molecular markers. PCR amplification of genomic DNA samples extracted from four *Asparagus officinalis* accessions (AO0012M, AO0606F, Glm002H and WC9), four *A. kiusianus* accessions (AK0101M, AK0301, AK0401 and AK0501), and an '*A. officinalis* × *A. kiusianus*' F_1 hybrid for (A) insertion/deletion (Indel), (B) simple sequence repeat (SSR), and (C) cleaved amplified polymorphic sequence (CAPS) markers. Restriction endonucleases used for CAPS markers are indicated.

Supplementary files

Table S1. Signal intensities of 1483 metabolites successfully assigned in *Asparagus kiusianus* (AK) and *A. officinalis* (AO) 24 and 48 h post-inoculated with *Phomopsis asparagi* (AKI_24 hpi, AKI_48 hpi, AOI_24 hpi and AOI_48 hpi) and non-inoculated controls (AKC and AOC) using negative ion mode on the basis of liquid chromatography-quadrupole time-of-flight mass spectrometry, retention time (RT), mass-to-charge (*m/z*).

Table S2. Signal intensities of 1239 metabolites successfully assigned in *Asparagus kiusianus* (AK) and *A. officinalis* (AO) 24 and 48 h post-inoculated with *Phomopsis asparagi* (AKI_24 hpi, AKI_48 hpi, AOI_24 hpi and AOI_48 hpi) and non-inoculated controls (AKC and AOC) using positive ion mode on the basis of liquid chromatography-quadrupole time-of-flight mass spectrometry, retention time (RT) and mass-to-charge (*m/z*).

Table S3. Signal/peak intensities of 14 metabolites successfully annotated and identified in *Asparagus kiusianus* (AK) and *A. officinalis* (AO) 24 and 48 h post-inoculated with *Phomopsis asparagi* (AKI_24 hpi, AKI_48 hpi, AOI_24 hpi and AOI_48 hpi) and non-inoculated controls (AKC and AOC) using positive and negative ion modes on the basis of tandem-mass spectrometry (MS/MS), exact mass number and retention time (RT) of authentic standards and literature. Out of 14 identified metabolites, 13 metabolites were differentially produced in at least one of the nine comparisons by the preset criteria. Red and blue numbers indicated increased (FC $\geq$ 2.0; $P < 0.05$) and decreased (FC $\leq$ 0.5; $P < 0.05$) fold changes of identified metabolites in comparisons.

Table S4. Fold change (FC) and false discovery rate (FDR) of differentially expressed genes in *Asparagus officinalis* 24 and 48 h post-inoculated (AOI_24 and 48 hpi) with *Phomopsis asparagi* in comparison with non-inoculated control plant (AOC).

Table S5. Fold change (FC) and false discovery rate (FDR) of differentially expressed genes in *Asparagus kiusianus* 24 and 48 h post-inoculated (AKI_24 and 48 hpi) with *Phomopsis asparagi* in comparison with non-inoculated control plant (AKC).

Table S6. Fold change (FC) and false discovery rate (FDR) of differentially expressed genes in *Asparagus kiusianus* 24 and 48 h post-inoculated (AKI_24 and 48 hpi) with *Phomopsis asparagi* in comparison with *A. officinalis* 24 and 48 hpi (AOI_24 hpi and AOI_48 hpi).

Table S7. List of the 211 core genes that are upregulated in the resistant *Asparagus kiusianus* 24 and 48 h post-inoculated with *Phomopsis asparagi* (AKI_24 and 48 hpi), and downregulated in the susceptible *A. officinalis* 24 and 48 hpi (AOI_24 and 48 hpi). Gene expression are represented by $\log_2$ (fold change). Preset fold change and false discovery rate ($\log_2$ (FC) ≥ 1 or $\log_2$ (FC) ≤ -1; FDR < 0.05) were used as minimum cutoffs.

Table S8. List of the primer pairs used for real-time quantitative PCR (RT-qPCR), and validation of the usefulness of the designed simple sequence repeat (SSR), insertion/deletion (Indel) and cleaved amplified polymorphic sequences (CAPS) markers.

Table S9. Gradient conditions for liquid chromatography-quadrupole time-of-flight mass spectrometry (LC-Q-TOF-MS) and tandem-mass spectrometry (MS/MS) analyses.

Figure S1. Principal component analysis (PCA) of metabolite signal intensities successfully assigned in susceptible cultivated *Asparagus officinalis* (AO) and resistant wild *A. kiusianus* (AK) plants 24 and 48 h post-inoculated with *Phomopsis asparagi* (AOI_24 hpi, AOI_48 hpi, AKI_24 hpi and AKI_48 hpi), and non-inoculated controls (AOC and AKC). (A-B) Loading plots of metabolite signal intensities detected by using positive (A) and negative (B) ion modes of liquid chromatography-quadrupole time-of-flight mass spectrometry (LC-Q-TOF-MS).

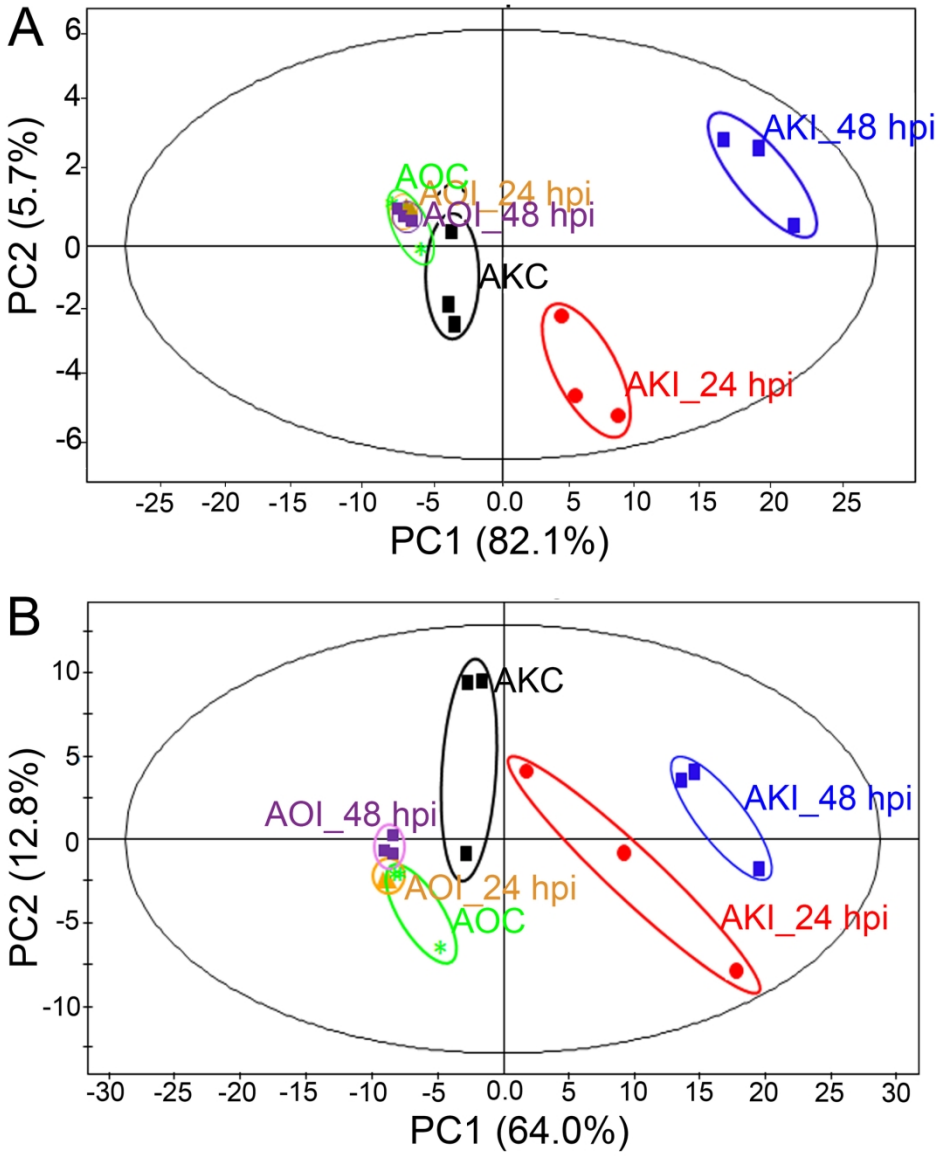

Fig. 1 Principal component analysis (PCA) of the assigned metabolite signal intensities obtained from the susceptible cultivated Asparagus officinalis (AO) and resistant wild A. kiusianus (AK) plants 24 and 48 h post-inoculated with Phomopsis asparagi (AOI_24 hpi, AOI_48 hpi, AKI_24 hpi and AKI_48 hpi), and non-inoculated controls (AOC and AKC). (A-B) Score plots of metabolite signal intensities detected by using positive (A) and negative (B) ion modes of liquid chromatography-quadrupole time-of-flight mass spectrometry (LC-Q-TOF-MS).

90x109mm (600 x 600 DPI)

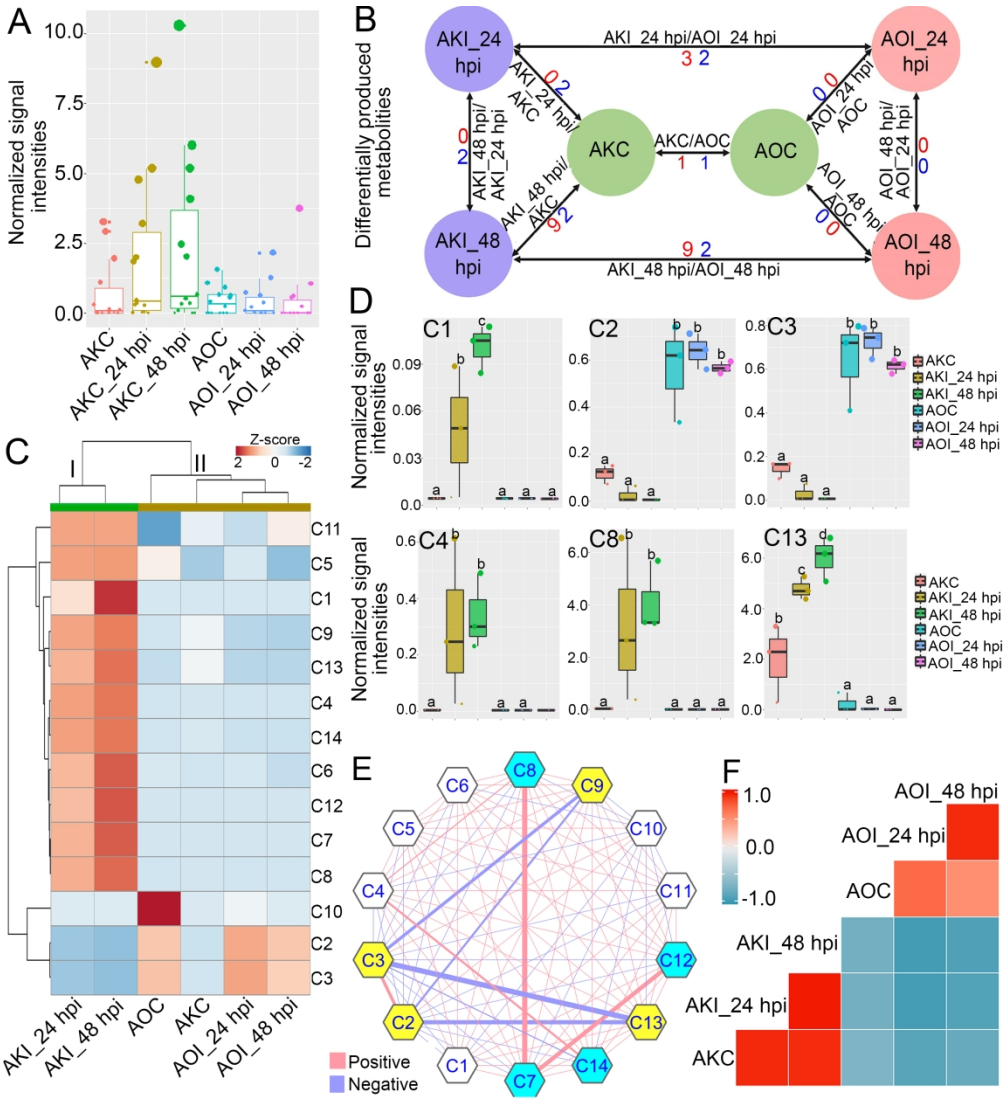

Fig. 2 Metabolite profiles and correlation analyses of susceptible Asparagus officinalis (AO) and resistant wild A. kiusianus (AK) plants 24 and 48 h post-inoculated with Phomopsis asparagi (AOI_24 hpi, AOI_48 hpi, AKI_24 hpi and AKI_48 hpi), and non-inoculated controls (AOC and AKC). (A) Boxplot of the signal intensities of 14 metabolites identified in the examined Asparagus species. (B) Venn diagram of the 13 differentially produced metabolites in the examined Asparagus species in response to P. asparagi. Red and blue numbers indicated increased (FC ≥ 2.0; $P < 0.05$) and decreased (FC ≤ 0.5; $P < 0.05$) metabolites. (C) Heatmap hierarchal clustering of the 14 metabolite signal intensities in the investigated Asparagus species using the Z-scores. (D) Boxplots of cyanidin-hex-dhex-hex (C1), cyanidin 3-rutinoside (C4), idaein (C8), furost-ene-triol-hex-dhex-hex (C13) and asparagusic acid glucose ester (C2 and C3) signal intensities, which exhibited higher and lower accumulations, respectively, in the examined Asparagus species. (E) Metabolite-metabolite correlation network. (F) Genotype-genotype correlations of the examined Asparagus species. Significant letters indicate significant differences between examined Asparagus species in response to P. asparagi at $P < 0.05$, according to a Duncan multiple range test.

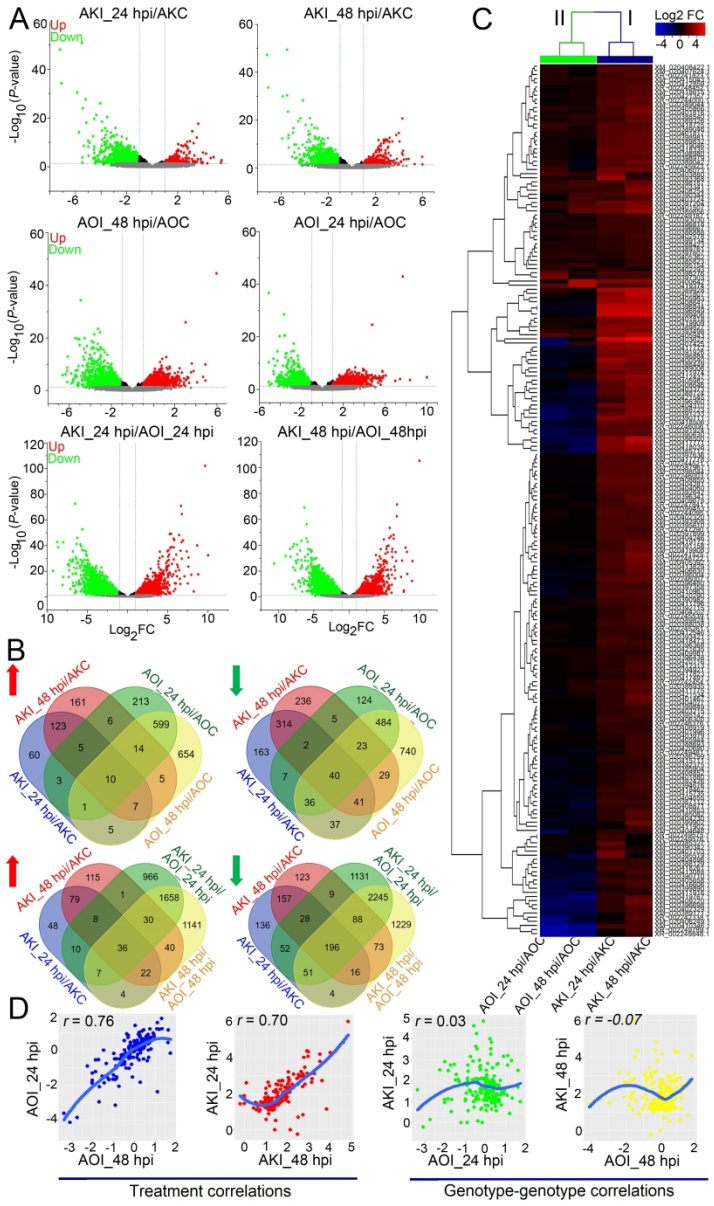

Fig. 3 Transcriptome profiles and correlation analyses of susceptible Asparagus officinalis (AO) and resistant wild A. kiusianus (AK) plants 24 and 48 h post-inoculated with Phomopsis asparagi (AOI_24 hpi, AOI_48 hpi, AKI_24 hpi and AKI_48 hpi), and non-inoculated controls (AOC and AKC). (A) Volcano plots of differentially expressed genes (DEGs) in the examined Asparagus species in response to P. asparagi. (B) Venn diagrams of overlapping DEGs in examined Asparagus species in response to P. asparagi. (C) Heatmap hierarchical clustering of 211 core genes upregulated in resistant wild AKI-24 hpi and/or AKI_48 hpi versus non-treated control AKC, and downregulated in susceptible AOI_24 hpi and/or AOI_48 hpi versus non-treated control AOC. (D) Treatment and genotype-genotype correlations based on the Pearson correlation coefficient of the 211 core genes.

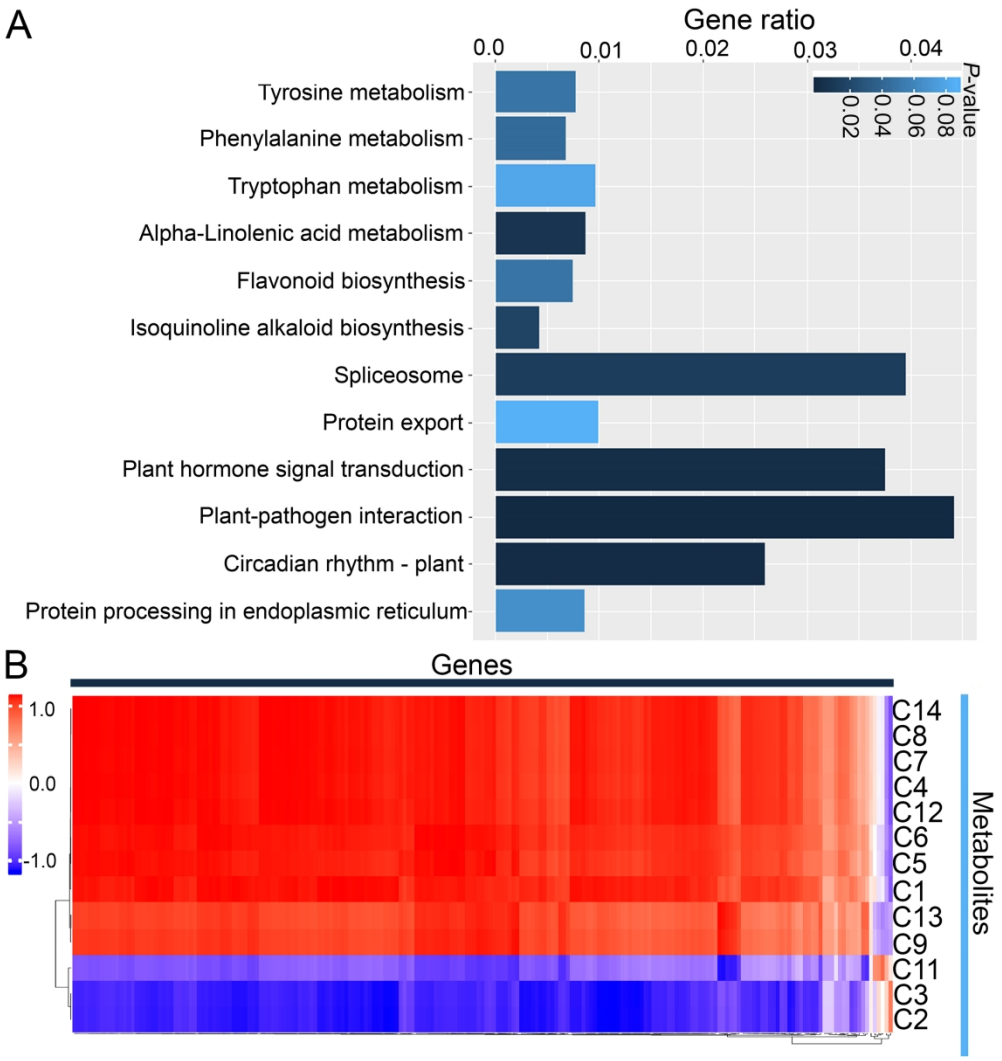

Fig. 4 Kyoto encyclopedia of genes and genomes (KEGG) enrichment analysis, and metabolite-gene correlation analysis. (A) KEGG enrichment analysis of 211 core genes that are upregulated in resistant wild A. kiusianus plants 24 and 48 h post-inoculated with Phomopsis asparagi (AKI_24 hpi and/or AKI_48 hpi) versus non-treated control AKC, and downregulated in susceptible A. officinalis (AOI_24 hpi and/or AOI_48 hpi) versus non-treated control AOC. (B) Correlation analysis of the 211 core genes and 13 differentially produced metabolites in the examined Asparagus species in response to P. asparagi.

119x130mm (600 x 600 DPI)

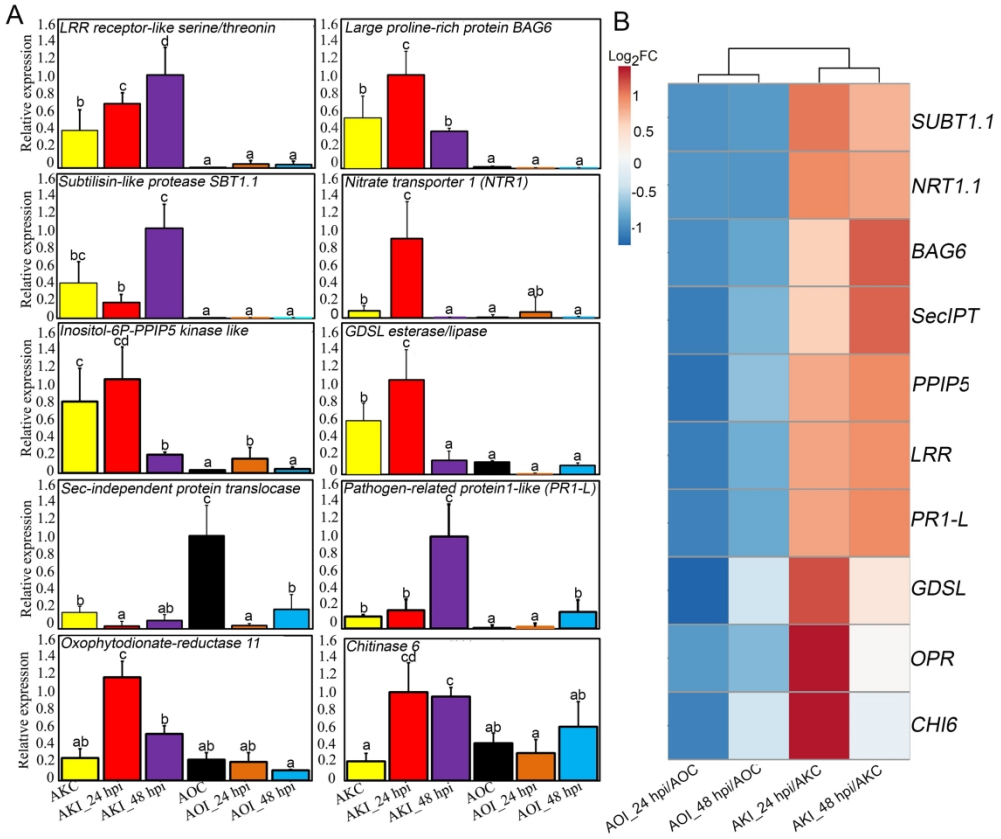

Fig. 5 Expression patterns of 10 representative genes in Asparagus officinalis (AO) and A. kiusianus (AK) plants 24 and 48 h post-inoculated with Phomopsis asparagi (AOI_24 hpi, AOI_48 hpi, AKI_24 hpi, and AKI_48 hpi) and non-inoculated controls (AOC and AKC). (A) Expression levels were quantified by real-time quantitative PCR (RT-qPCR). (B) Fold changes in gene expression derived from the RNA-seq were used to generate the heatmap. Values represent the means of three independent biological replicates and standard deviations (n = 3). Different letters indicate significant differences among various treatments according to a Tukey's HSD.

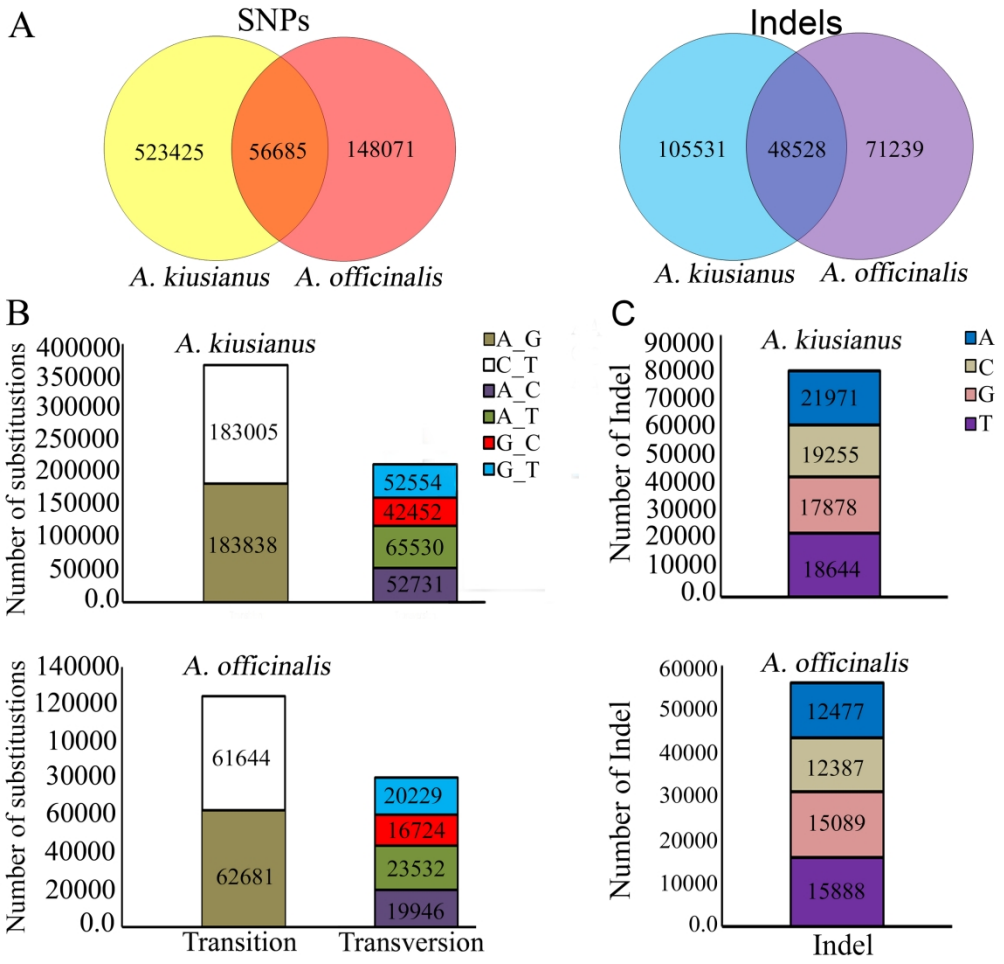

Fig. 6 Single nucleotide polymorphism (SNP) and insertion/deletion (Indel) distributions in Asparagus officinalis and A. kiusianus transcriptome datasets. (A) Venn diagrams showing the distributions of overlapping SNPs and Indels in A. officinalis and A. kiusianus compared with the A. officinalis reference genome Aspof.V1. (B–C) Total number of transition-type and transversion-type SNPs (B), and Indel distribution (C) in A. officinalis and A. kiusianus transcriptomes. A_G, A-to-G; C_T, C-to-T; A_C, A-to-C; A_T, A-to-T; G_C, G-to-C; G_T, G-to-T.

130x130mm (600 x 600 DPI)

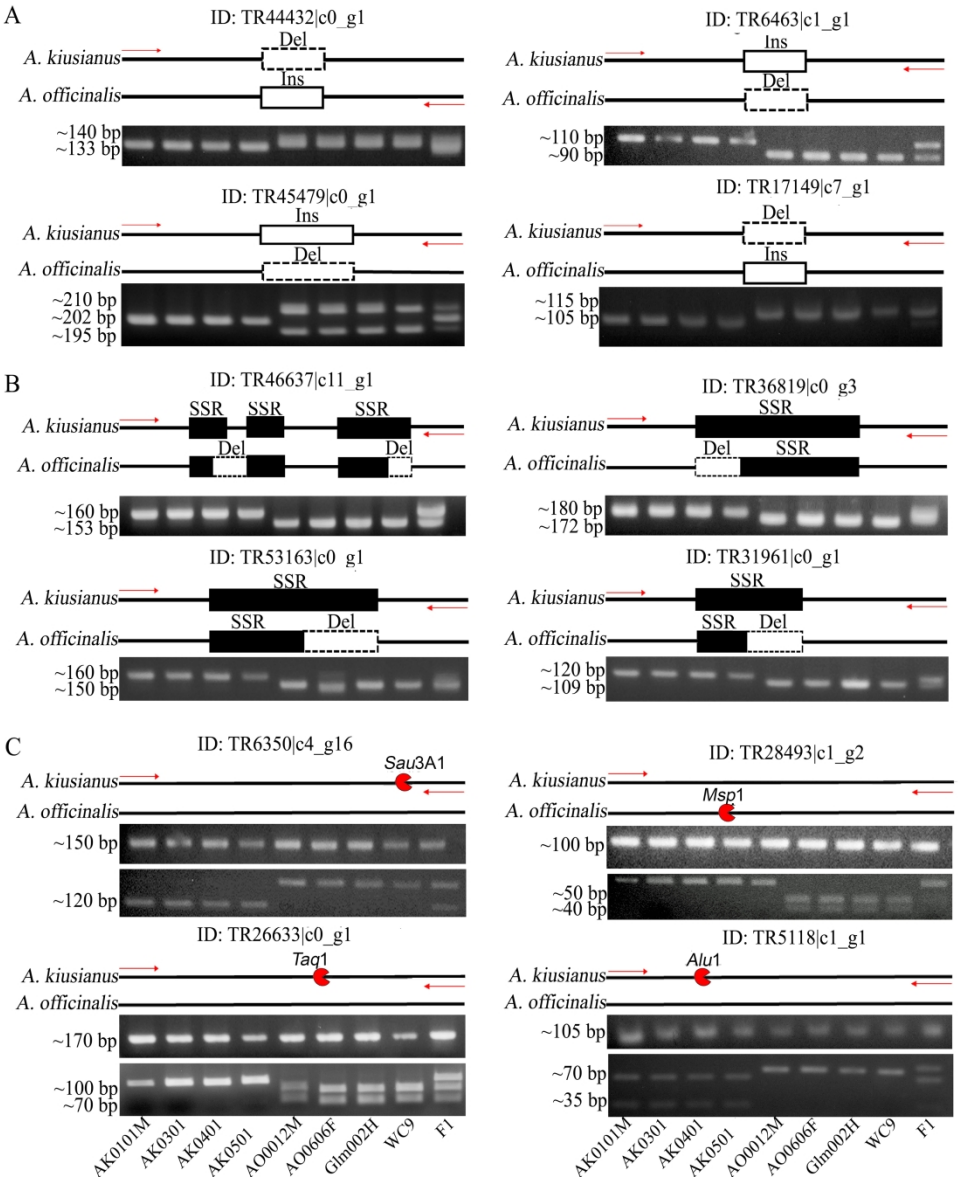

Fig. 7 Verification and discrimination of examined Asparagus species using the designed molecular markers. PCR amplification of genomic DNA samples extracted from four Asparagus officinalis accessions (AO0012M, AO0606F, Glm002H and WC9), four A. kiusianus accessions (AK0101M, AK0301, AK0401 and AK0501), and an 'A. officinalis × A. kiusianus' F1 hybrid for (A) insertion/deletion (Indel), (B) simple sequence repeat (SSR), and (C) cleaved amplified polymorphic sequence (CAPS) markers. Restriction endonucleases used for CAPS markers are indicated.